

Novel rhenium(III) complexes with 5,6-diphenyl-3-(2-pyridyl)-1,2,4-triazine: X-ray structures and DFT calculations for $[\text{ReCl}_3(\text{OPPh}_3)(\text{dppt})]$ and $[\text{ReCl}_3(\text{PPh}_3)(\text{dppt})]$ complexes

B. Machura^{a,*}, R. Kruszynski^b, J. Kusz^c, J. Kłak^d, J. Mroziński^d

^a Department of Inorganic and Coordination Chemistry, Institute of Chemistry, University of Silesia, 9th Szkolna Street, 40-006 Katowice, Poland

^b Department of X-ray Crystallography and Crystal Chemistry, Institute of General and Ecological Chemistry, Lodz University of Technology, 116 Żeromski Street, 90-924 Łódź, Poland

^c Institute of Physics, University of Silesia, 4th Uniwersytecka Street, 40-006 Katowice, Poland

^d Faculty of Chemistry, Wrocław University, F. Joliot-Curie 14 Street, 50-383 Wrocław, Poland

Received 20 March 2007; accepted 31 May 2007

Available online 15 June 2007

Abstract

The reaction of $[\text{ReOCl}_3(\text{PPh}_3)_2]$ with 5,6-diphenyl-3-(2-pyridyl)-1,2,4-triazine (dppt) has been examined and $[\text{ReCl}_3(\text{OPPh}_3)(\text{dppt})]$ has been obtained. The triphenylphosphine oxide can be easily replaced by PPh_3 in the reaction of $[\text{ReCl}_3(\text{OPPh}_3)(\text{dppt})]$ with an excess of triphenylphosphine. The $[\text{ReCl}_3(\text{OPPh}_3)(\text{dppt})]$ and $[\text{ReCl}_3(\text{PPh}_3)(\text{dppt})]$ complexes have been structurally and spectroscopically characterized. Their molecular orbital diagrams have been calculated with the density functional theory (DFT) method, and their electronic spectra have been discussed on the basis of time-dependent DFT calculations. The compound $[\text{ReCl}_3(\text{OPPh}_3)(\text{dppt})]$ has been studied additionally by magnetic measurement. The magnetic behavior is characteristic of mononuclear complexes with d^4 low-spin octahedral Re(III) complexes ($^3T_{1g}$ ground state) and arise because of the large spin–orbit coupling ($\zeta = 2500 \text{ cm}^{-1}$), which gives diamagnetic ground state.

© 2007 Elsevier Ltd. All rights reserved.

Keywords: Rhenium complexes; 6-Diphenyl-3-(2-pyridyl)-1,2,4-triazine; X-ray and electronic structure; DFT calculations; Magnetic measurement

1. Introduction

For many years inorganic compounds containing an oxygen atom multiply bonding to a transition metal have been in the centre of interest to those scientists engaged in basic research and to those trying to employ these complexes in catalytic processes. Oxygen atom transfer chemistry has been implicated in various reactions of industrial

and biological importance, including olefin epoxidation and catalysis by cytochrome P-450 [1–3].

The chemistry of oxo rhenium complexes arouses particular interest among these compounds. It results from the favourable nuclear properties of ^{186}Re and ^{188}Re nuclides, which make the radioisotopes useful for diagnostic nuclear medicine and applications in radioimmunotherapy [4,5].

In this context, the design, synthesis and reactivity of rhenium oxocomplexes has become the aim of several laboratories, including ours.

Previously, we investigated the reactivity of oxorhenium(V) species – $[\text{ReO}(\text{OEt})\text{X}_2(\text{PPh}_3)_2]$, $[\text{ReOX}_3(\text{PPh}_3)_2]$ and $[\text{ReOX}_3(\text{AsPh}_3)(\text{OAsPh}_3)]$ ($\text{X} = \text{Cl}$ or Br) – towards pyrazole, 3,5-dimethylpyrazole and benzotriazole [6].

* Corresponding author.

E-mail addresses: basia@ich.us.edu.pl (B. Machura), rafal.kruszynski@p.lodz.pl (R. Kruszynski), jmroz@wchuwr.chem.uni.wroc.pl (J. Mroziński).

In this report we focus on the examination of the reaction of $[\text{ReOCl}_3(\text{PPh}_3)_2]$ with 5,6-diphenyl-3-(2-pyridyl)-1,2,4-triazine (dppt). The isolated $[\text{ReCl}_3(\text{OPPh}_3)(\text{dppt})]$ complex easily reacts with an excess of triphenylphosphine to give $[\text{ReCl}_3(\text{PPh}_3)(\text{dppt})]$. The last one can be also prepared in the reaction of $[\text{ReCl}_3(\text{MeCN})(\text{PPh}_3)_2]$ with 5,6-diphenyl-3-(2-pyridyl)-1,2,4-triazine. Here we present spectroscopic characterization, crystal, molecular and electronic structure of $[\text{ReCl}_3(\text{OPPh}_3)(\text{dppt})]$ (**1**) and $[\text{ReCl}_3(\text{PPh}_3)(\text{dppt})]$ (**2**) complexes. The molecular orbital diagrams of **1** and **2** have been calculated with the density functional theory (DFT) method. Currently density functional theory (DFT) is commonly used to examine the electronic structure of transition metal complexes. It meets with the requirements of being accurate, easy to use and fast enough to allow the study of relatively large molecules of transition metal complexes [7]. The electronic spectra of **1** and **2** have been discussed on the basis of time-dependent DFT calculations. Recent studies have supported the TD-DFT method to be applicable for open- and closed-shell of 5d-metal complexes (including rhenium complexes) giving good assignment of experimental spectra [8–10].

2. Experimental

2.1. General procedure

The reagents used to the synthesis were commercially available and were used without further purification. The $[\text{ReOCl}_3(\text{PPh}_3)_2]$ complex was prepared according to the literature method [11].

IR spectra were recorded on a Nicolet Magna 560 spectrophotometer in the spectral range $4000\text{--}400\text{ cm}^{-1}$ with the samples in the form of KBr pellets. Electronic spectra were measured on a spectrophotometer Lab Alliance UV–VIS 8500 in the range $1000\text{--}200\text{ nm}$ in chloroform solution. Elemental analyses (C, H, N) were performed on a Perkin–Elmer CHN-2400 analyzer.

2.2. Preparation of $[\text{ReCl}_3(\text{OPPh}_3)(\text{dppt})] \cdot \text{CH}_2\text{Cl}_2$ (**1** · CH_2Cl_2)

To a solution of $[\text{ReOCl}_3(\text{PPh}_3)_2]$ (0.50 g, 0.6 mmol) in 30 ml dichloromethane was added 0.19 g (0.61 mmol) of 5,6-diphenyl-3-(2-pyridyl)-1,2,4-triazine (dppt). The resulting solution was magnetically stirred for 2 h at room temperature, and during this time the colour changed from light green to violet. 20 ml of CH_2Cl_2 was distilled off and 50 ml of diethyl ether was added. $[\text{ReCl}_3(\text{OPPh}_3)(\text{dppt})] \cdot \text{CH}_2\text{Cl}_2$ was filtered off, washed with ethanol, diethyl ether and dried (yield 90%). The dark violet crystals of **1** · CH_2Cl_2 for X-ray investigation were obtained by recrystallization from dichloromethane.

IR (KBr; ν/cm^{-1}): 1601 (m), 1590(m) and 1504 (m) ν_{CN} and $\nu_{\text{C}=\text{C}}$; 1141(s) and 1115(s) $\nu_{\text{P}=\text{O}}$.

Anal. Calc. for $\text{C}_{39}\text{H}_{31}\text{Cl}_5\text{N}_4\text{OPRe}$: C, 48.48; H, 3.23; N, 5.80. Found: C, 48.60; H, 3.18; N, 5.85%.

2.3. Preparation of $[\text{ReCl}_3(\text{PPh}_3)(\text{dppt})]$ (**2**)

Method A: To a solution of complex **1** (0.20 g, 0.23 mmol) in chloroform (20 ml), PPh_3 (0.24 g, 0.92 mmol) was added and the solution was refluxed for 1 h. The solvent was then removed under reduced pressure. The precipitate was washed several times with ethanol and hexane, and finally dried *in vacuo*. The crystals of **2** suitable for X-ray investigation were obtained by recrystallization from chloroform (yield 95%).

Method B: $[\text{Re}(\text{MeCN})\text{Cl}_3(\text{PPh}_3)_2]$ (0.5 g, 0.58 mmol) and dppt (0.19 g, 0.61 mmol) in chloroform (40 cm^3) were refluxed for 4 h. The starting material gradually dissolved and the colour of the reaction solution became dark red. The volume was condensed to 10 cm^3 , diethyl ether (100 cm^3) was added and dark violet microcrystalline solid was filtered. The product was washed with EtOH and cold ether, and dried *in vacuo* (yield 90%).

IR (KBr; ν/cm^{-1}): 1599(m), 1572(w) and 1507 (w) ν_{CN} and $\nu_{\text{C}=\text{C}}$.

Anal. Calc. for $\text{C}_{38}\text{H}_{29}\text{Cl}_3\text{N}_4\text{PRe}$: C, 52.75; H, 3.38; N, 6.48. Found: C, 52.62; H, 3.45; N, 6.37%.

2.4. Crystal structures determination and refinement

The X-ray intensity data of **1** · CH_2Cl_2 and **2** were collected on a KM-4-CCD automatic diffractometer equipped with CCD detector and graphite-monochromated Mo K α radiation ($\lambda = 0.71073\text{ \AA}$) at room temperature. Details concerning crystal data and refinement are given in Table 1. Lorentz polarization and absorption correction [12] were applied. The structures were solved by the Patterson method and subsequently completed by the difference Fourier recycling. All the non-hydrogen atoms were refined anisotropically using full-matrix, least-squares technique. The hydrogen atoms were treated as “riding” on their parent carbon atoms and assigned isotropic temperature factors equal 1.2 times the value of equivalent temperature factor of the parent atom. SHELXS-97 [13], SHELXL-97 [14] and SHELXTL [15] programs were used for all the calculations. Atomic scattering factors were those incorporated in the computer programs.

2.5. Computational details

GAUSSIAN-03 program [16] was used in the calculations. The geometry optimizations of **1** and **2** were carried out with the DFT method with the use of B3LYP functional [17,18]. The electronic spectra of **1** and **2** were calculated with the TD-DFT method [19]. The calculations were performed by using ECP basis set on the rhenium atom, the standard 6-31+G** basis for chlorine, oxygen, and nitrogen, 6-31G* for carbon and 6-31G for hydrogen atoms. The Xe core electrons of Re were replaced by an effective core potential and DZ quality Hay and Wadt Los Alamos ECP basis set (LANL2DZ) [20] was used for the valence electrons. Additional *d* function with exponent $\alpha = 0.3811$

Table 1
Crystal data and structure refinement for complexes **1** and **2**

Compound	1 · CH ₂ Cl ₂	2
Empirical formula	C ₃₉ H ₃₁ Cl ₅ N ₄ OPRe	C ₃₈ H ₂₉ Cl ₃ N ₄ PRe
Formula weight	966.10	865.17
Temperature (K)	291.0(3)	295(2)
Wavelength (Å)	0.71073	0.71073
Crystal system	monoclinic	monoclinic
Space group	<i>P</i> 2 ₁ / <i>c</i>	<i>P</i> 2 ₁ / <i>c</i>
<i>Unit cell dimensions</i>		
<i>a</i> (Å)	9.7664(4)	10.2122(4)
<i>b</i> (Å)	18.9933(8)	12.1143(3)
<i>c</i> (Å)	21.7652(8)	28.2982(12)
β (°)	94.151(3)	90.834(3)
Volume (Å ³)	4026.8(3)	3500.5(2)
<i>Z</i>	4	4
<i>D</i> _{calc} (Mg/m ³)	1.594	1.642
Absorption coefficient (mm ⁻¹)	3.425	3.780
<i>F</i> (000)	1904	1704
Crystal size (mm)	0.13 × 0.28 × 0.50	0.03 × 0.08 × 0.30
θ Range for data collection (°)	2.91–25.11	2.97–25.00
Index ranges	–11 ≤ <i>h</i> ≤ 11, –22 ≤ <i>k</i> ≤ 22, –25 ≤ <i>l</i> ≤ 25	–11 ≤ <i>h</i> ≤ 6, –14 ≤ <i>k</i> ≤ 7, –26 ≤ <i>l</i> ≤ 33
Reflections collected	42201	10927
Independent reflections (<i>R</i> _{int})	7169 (0.0575)	6168 (0.0374)
Completeness to 2 θ (%)	99.5	99.9
Maximum and minimum transmission	0.586 and 0.260	0.888 and 0.711
Data/restraints/parameters	7169/0/460	6168/0/424
Goodness-of-fit on <i>F</i> ²	1.116	0.893
Final <i>R</i> indices [<i>I</i> > 2 σ (<i>I</i>)]	<i>R</i> ₁ = 0.0338, <i>wR</i> ₂ = 0.0788	<i>R</i> ₁ = 0.0279, <i>wR</i> ₂ = 0.0439
<i>R</i> indices (all data)	<i>R</i> ₁ = 0.0389, <i>wR</i> ₂ = 0.0815	<i>R</i> ₁ = 0.0555, <i>wR</i> ₂ = 0.0462
Largest difference in peak and hole (e Å ⁻³)	1.358 and –0.803	1.013 and –0.815

and *f* function with exponent $\alpha = 2.033$ on the rhenium atom were added.

2.6. Magnetic measurement

Magnetic measurements in the temperature range 1.8–300 K were performed using a Quantum Design SQUID-based MPMSXL-5-type magnetometer. The SQUID magnetometer was calibrated with the palladium rod sample (Materials Research Corporation, measured purity 99.9985%). The superconducting magnet was generally operated at a field strength ranging from 0 to 5 T. Measurements were made at a magnetic field of 0.5 T. Corrections are based on subtracting the sample – holder signal and contribution χ_D estimated from the Pascal constants [21] and equal $-425 \times 10^{-6} \text{ cm}^3 \text{ mol}^{-1}$ for complex [ReCl₃(OPPh₃)(dppt)]. The effective magnetic moment was calculated from the equation, $\mu_{\text{eff}} = 2.83(\chi_{\text{M}}T)^{1/2}$ (BM).

3. Results and discussion

3.1. Preparation and infrared data

The [ReCl₃(dppt)(OPPh₃)] (**1**) complex has been prepared in good yield in the reaction of [ReOCl₃(PPh₃)₂] with 5,6-diphenyl-3-(2-pyridyl)-1,2,4-triazine (dppt) in dichloromethane:



It can be supposed that the [ReOCl₃(dppt)] oxocompound, formed in the first step reaction, is an oxidant transferring an oxygen atom to PPh₃. The oxygen atom transfer is believed to proceed *via* initial nucleophilic attack on the Re≡O π^* orbitals, the π acidity of the dppt ligand facilitates the attack of triphenylphosphine [22]. The produced triphenylphosphine oxide remains bonded to the reduced rhenium ion in complex **1**. Many instances of formation of phosphine oxides from Re^VO and tertiary phosphines can be given, but examples when the phosphine oxide remain firmly bonded to the reduced metal centre are rare [22–25]. The complex **1** easily reacts with an excess of PPh₃ to give [ReCl₃(dppt)(PPh₃)] (**2**). The last one has been also isolated in the reaction of [ReCl₃(MeCN)(PPh₃)₂] with dppt.

The elemental analyses of the **1** · CH₂Cl₂ and **2** complexes are in good agreement with their formulation. The characteristic bands corresponding to the $\nu(\text{CN})$, $\nu(\text{C}=\text{C})$ modes of the dppt ligand appear in the range 1610–1500 cm⁻¹ in the IR spectrum of **1** and **2**. The absence of the characteristic strong $\nu(\text{Re}=\text{O})$ band at $\sim 980 \text{ cm}^{-1}$ is clear indication that there is no oxo-Re(V) starting material left in the samples **1** and **2**. The strong bands at 1141 and 1115 cm⁻¹ in the IR spectrum of **1** confirm the presence of the coordinated OPPh₃ molecule [26].

3.2. Crystal structures

The complex **1** crystallises as dichloromethane solvate **1** · CH₂Cl₂, and the dichloromethane molecule is not bonded to any atom of the Re(III) complex. The structure of **2** consist of discrete and well-separated [ReCl₃(dppt)(PPh₃)] monomers. Any intermolecular interactions with enough strength to govern crystal packing or molecule conformation were not found in the structures of **1** and **2**. Only weak intramolecular and intermolecular hydrogen bonds [25–27] were detected in crystals **1** and **2**, and they are gathered in Table 2.

The molecular structures of **1** and **2** are presented in Figs. 1 and 2, respectively, and the selected bond distances and angles are collected in Tables 3 and 4, respectively. Both complexes show distorted octahedral geometry about Re with the three chloride ions arranged in *meridional* fashion in complex **1** and in *facial* configuration in complex **2**. The coordination polyhedron least squares planes are inclined at 88.54(6)°, 82.95(11)°, and 74.58(13)° in compound **1** and at 89.05(5)°, 86.90(8)°, and 87.87(5)° in

Table 2
Hydrogen bonds for **1** and **2**

D	A	$d(\text{H}\cdots\text{A})$ (Å)	$d(\text{D}\cdots\text{A})$ (Å)	$\angle\text{D-H}\cdots\text{A}$ (°)
<i>Compound 1</i>				
C(6)	Cl(3)#1	2.81	3.467(4)	129.1
C(8)	Cl(1)#2	2.80	3.655(5)	153.5
C(30)	Cl(2)#3	2.77	3.593(7)	147.5
<i>Compound 2</i>				
C(9)	Cl(3)#4	2.73	3.562(6)	149.2

Symmetry codes: #1: $1-x, -y, -z$; #2: $-x, -y, -z$; #3: $-1+x, y, z$; #4: $-x, y-1/2, -z+1/2$.

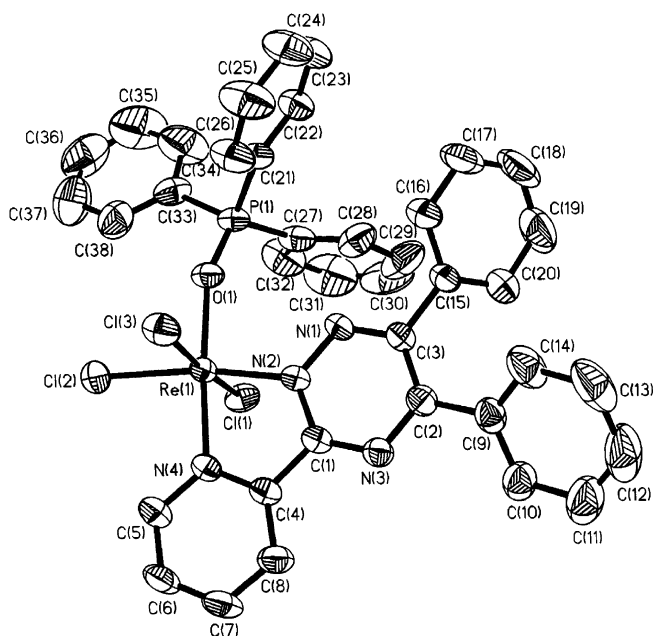


Fig. 1. The molecular structure of **1**.

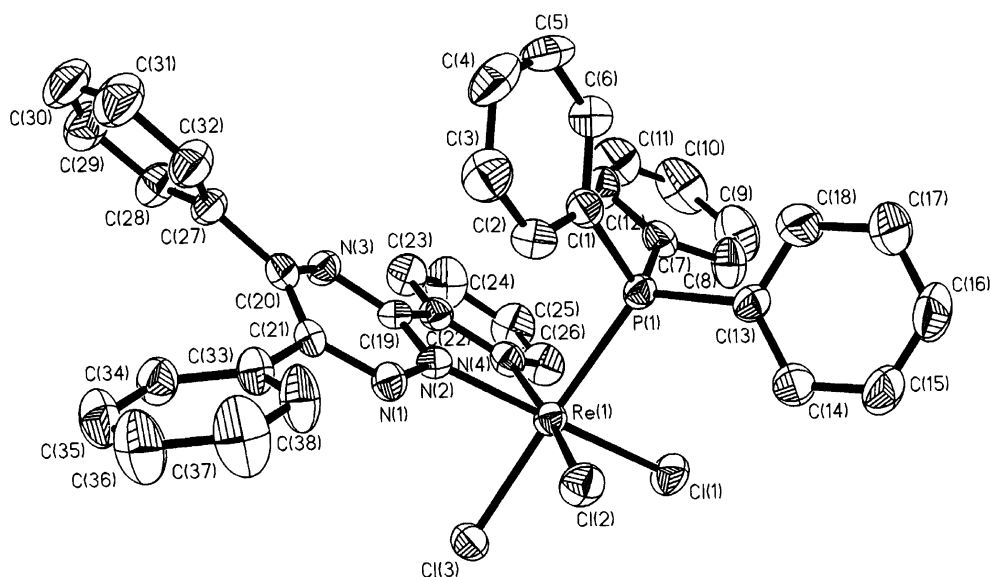


Fig. 2. The molecular structure of **2**.

compound **2** what shows that polyhedron distortion is distinctly smaller in compound **2**. The OPPh_3 ligand is pure donor and $\text{PPh}_3\text{P}=\text{O} \rightarrow \text{Re} \rightarrow \pi^*(\text{dppt})$ interaction is suited to the *meridional* configuration. In the presence of PPh_3 the electronic situation is affected by π acidity of the phosphine ligand. In complex **2**, two good π acceptor, dppt and PPh_3 , are coordinated to rhenium (III) centre, and the back-bonding effect is maximized in the *facial* disposition which ensures minimum competition between the two ligands for identical metal orbitals. It is significant that the Re-N distances in **2** are longer than those in **1** where the dppt ligand alone is available for back bonding. The presence of Re-PPh_3 back-bonding diminishes the demand on $\pi^*(\text{dppt})$ orbitals. Some differences are observed between the $\text{Re-N}(\text{pyridine})$ and $\text{Re-N}(\text{triazine})$ bond lengths in **1** and **2** complexes. It indicates different π acidity strength of the two rings – the triazine ring favours π -back donation from the rhenium ion. Nevertheless, the Re-N bond lengths of both complexes are similar to those found for the other rhenium(III) polypyridyl compounds: in $[\text{ReCl}_2(\text{bipy})_2]\text{PF}_6$ – 2.094(5) and 2.096(5) Å [27] and in the $[\text{ReL}(\text{terpy})_2]^{2+}$ ($\text{L} = \text{Cl}, \text{OH}, \text{NCS}$) complexes – about 2.10 Å [28]. These values are significantly shorter than comparable distances for saturated amine complexes, where metal-to-ligand π -back bonding is not possible, for instance, the Re-NH_2 distance in the $[\text{Re}(\text{N}_2)(\text{ampy})-(\text{tbpy})(\text{PPh}_3)]\text{PF}_6$ compound is 2.197(7) [29].

The $\text{Re-Cl}(3)$ distance of **2** is affected by *trans* influence of triphenylphosphine and is therefore longer than the $\text{Re-Cl}(1)$ and $\text{Re-Cl}(2)$ bond lengths located in *trans* positions to the dppt ligand. In both compounds the 3-(2-pyridyl)-1,2,4-triazine moiety is close to planarity (maximum least squares plane atom deviation of 0.073(3) Å exists for C(2) atom in compound **1** and of 0.122(3) Å exists for N(4) atom in compound **2**). The dppt phenyl rings are

Table 3
The experimental and optimized bond lengths (Å) and angles (°) for **1**

Bond lengths	Experimental	Optimized	Bond angles	Experimental	Optimized
Re(1)–O(1)	2.054(3)	2.06	N(2)–Re(1)–O(1)	98.22(12)	96.26
Re(1)–N(2)	2.016(3)	2.03	N(2)–Re(1)–N(4)	76.94(12)	77.18
Re(1)–N(4)	2.068(3)	2.08	O(1)–Re(1)–N(4)	175.15(12)	173.38
Re(1)–Cl(1)	2.3664(11)	2.42	N(2)–Re(1)–Cl(1)	90.34(9)	90.32
Re(1)–Cl(2)	2.3900(11)	2.42	O(1)–Re(1)–Cl(1)	89.31(8)	90.00
Re(1)–Cl(3)	2.3856(11)	2.43	N(4)–Re(1)–Cl(1)	90.95(9)	90.91
			N(2)–Re(1)–Cl(3)	89.54(9)	89.78
			O(1)–Re(1)–Cl(3)	86.32(8)	87.09
			N(4)–Re(1)–Cl(3)	93.34(9)	91.95
			Cl(1)–Re(1)–Cl(3)	175.57(4)	177.09
			N(2)–Re(1)–Cl(2)	171.34(9)	171.97
			O(1)–Re(1)–Cl(2)	90.43(9)	91.76
			N(4)–Re(1)–Cl(2)	94.41(10)	94.79
			Cl(1)–Re(1)–Cl(2)	89.57(4)	90.03
			Cl(3)–Re(1)–Cl(2)	91.22(4)	90.27

Table 4
The experimental and optimized bond lengths (Å) and angles (°) for **2**

Bond lengths	Experimental	Optimized	Bond angles	Experimental	Optimized
Re(1)–P(1)	2.4505(11)	2.54	N(2)–Re(1)–N(4)	75.91(15)	76.26
Re(1)–N(2)	2.044(4)	2.06	N(2)–Re(1)–Cl(2)	95.36(11)	94.28
Re(1)–N(4)	2.117(4)	2.13	N(4)–Re(1)–Cl(2)	171.27(10)	170.52
Re(1)–Cl(1)	2.3600(13)	2.43	N(2)–Re(1)–Cl(1)	168.43(11)	168.39
Re(1)–Cl(2)	2.3386(14)	2.38	N(4)–Re(1)–Cl(1)	92.73(11)	92.18
Re(1)–Cl(3)	2.4009(10)	2.42	Cl(2)–Re(1)–Cl(1)	95.98(5)	97.26
			N(2)–Re(1)–Cl(3)	87.58(9)	87.97
			N(4)–Re(1)–Cl(3)	88.48(9)	86.20
			Cl(2)–Re(1)–Cl(3)	90.85(4)	92.85
			Cl(1)–Re(1)–Cl(3)	89.95(4)	90.21
			N(2)–Re(1)–P(1)	94.53(9)	96.73
			N(4)–Re(1)–P(1)	91.24(9)	94.45
			Cl(2)–Re(1)–P(1)	89.77(4)	87.28
			Cl(1)–Re(1)–P(1)	87.82(4)	85.09
			Cl(3)–Re(1)–P(1)	177.73(4)	175.27

inclined to the 3-(2-pyridyl)-1,2,4-triazine moiety at 37.95(16)° and 50.37(16)° in compound **1** and at 32.37(13)° and 39.62(16)° in compound **2**.

3.3. Geometry optimization

The geometries of **1** and **2** were optimized in triplet and singlet states using the DFT method with the B3LYP functional. The energies of the singlet states are of 15.2 and 15.7 kcal/mol higher for **1** and **2**, respectively. The optimized geometric parameters of the triplet states are gathered in Tables 3 and 4. In general, the predicted bond lengths and angles are in agreement with the values based upon the X-ray crystal structure data, and the general trends observed in the experimental data are well reproduced in the calculations.

3.4. Molecular orbitals

The energies and characters of several highest occupied and lowest unoccupied molecular orbitals of **1** and **2** are

presented in Tables 5 and 6. The selected HOMO and LUMO orbitals of **1** and **2** with α spin are depicted in Figs. 3 and 4. Among the highest occupied MOs of **1** and **2**, the largest numbers constitute π orbitals of the dppt and phenyl rings of PPh₃ or OPPh₃ with a contribution from the Cl and O (for **1**) atoms. For both **1** and **2**, the highest molecular orbital with α -spin can be represented as a combination of $\pi_{\text{Re-Cl}}^*$ and π_{dppt}^* , with predominant involvement of the former component. The same character have the HOMO orbitals with β -spin of **1** and **2**, but contribution of π orbitals of dppt ligand is considerable larger. The H-2 and H-1 α molecular orbitals of **1** correspond to combination of $\pi_{\text{Re-Cl}}^*$ and $\pi_{\text{Re-OPPh}_3}^*$ interaction, whereas the H-2 and H-1 α molecular orbitals of **2** have $\pi_{\text{Re-Cl}}^*$ character. To a large extent, the L + 1 and L + 3 β orbitals of **1** and L and L + 2 β orbitals of **2** are also formed by rhenium d_{π} atomic orbital (d_{xz} , d_{yz} or d_{xy}). Among the lowest unoccupied MOs of **1** and **2**, the largest numbers constitute π orbitals of the dppt and phenyl rings of PPh₃ or OPPh₃. For both complexes the LUMO and LUMO + 1 with α -spin have π^* (dppt) character. The π^* phenyl ring orbitals

Table 5
The energy and character of the selected molecular orbitals with α and β spins for **1**

	MOs with α spin		MOs with β spin	
	E (eV)	Character	E (eV)	Character
HOMO – 2	–6.065	$d_{xy}(\text{Re})$, $\pi(\text{Cl})$, $\pi(\text{O})$	–6.840	$\pi(\text{dppt})$, $\pi(\text{Cl})$
HOMO – 1	–5.622	$d_{xz}(\text{Re})$, $\pi(\text{Cl})$, $\pi(\text{O})$	–6.475	$\pi(\text{Cl})$
HOMO	–5.399	$d_{yz}(\text{Re})$, $\pi(\text{Cl})$, $\pi^*(\text{dppt})$	–4.566	$d_{xz}(\text{Re})$, $\pi(\text{Cl})$, $\pi^*(\text{dppt})$
LUMO	–2.520	$\pi^*(\text{dppt})$	–2.754	$\pi^*(\text{dppt})$, $d_{xz}(\text{Re})$
LUMO + 1	–2.331	$\pi^*(\text{dppt})$	–2.556	$d_{xy}(\text{Re})$, $\pi(\text{Cl})$, $\pi(\text{O})$
LUMO + 2	–1.624	$\pi^*(\text{Ph}_{\text{OPPh}_3})$	–2.359	$\pi^*(\text{dppt})$, $d_{xz}(\text{Re})$
LUMO + 3	–1.471	$\pi^*(\text{Ph}_{\text{OPPh}_3})$	–2.086	$d_{yz}(\text{Re})$, $\pi^*(\text{dppt})$

Table 6
The energy and character of the selected molecular orbitals with α and β spins for **2**

	MOs with α spin		MOs with β spin	
	E (eV)	Character	E (eV)	Character
HOMO – 2	–5.721	$d_{xy}(\text{Re})$, $\pi(\text{Cl})$	–6.417	$\pi(\text{Cl})$, $n(\text{P})$
HOMO – 1	–5.680	$d_{xz}(\text{Re})$, $\pi(\text{Cl})$	–6.403	$\pi(\text{Cl})$, $n(\text{P})$, $\pi(\text{Ph}_{\text{PPh}_3})$
HOMO	–5.515	$d_{yz}(\text{Re})$, $\pi(\text{Cl})$	–4.851	$d_{yz}(\text{Re})$, $\pi(\text{Cl})$, $\pi^*(\text{dppt})$
LUMO	–2.647	$\pi^*(\text{dppt})$	–2.904	$d_{xz}(\text{Re})$, $\pi^*(\text{dppt})$, $\pi(\text{Cl})$
LUMO + 1	–2.411	$\pi^*(\text{dppt})$	–2.577	$\pi^*(\text{dppt})$, d_{yz}
LUMO + 2	–1.448	$\pi^*(\text{dppt})$	–2.467	$d_{xy}(\text{Re})$, $\pi(\text{Cl})$
LUMO + 3	–1.098	$\pi^*(\text{Ph}_{\text{PPh}_3})$, $d_{z^2}(\text{Re})$	–2.295	$\pi^*(\text{dppt})$, d_{yz}

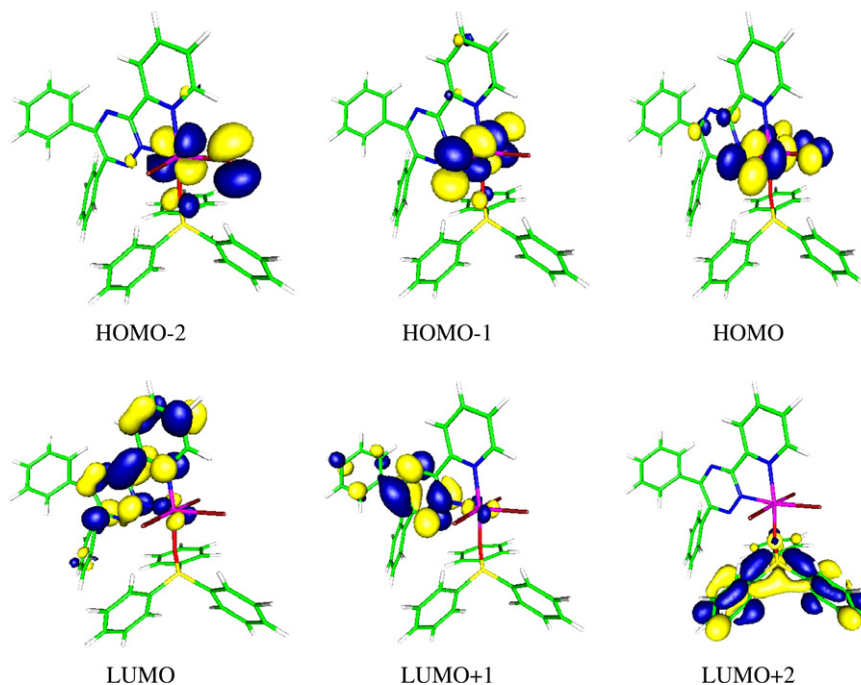


Fig. 3. The selected HOMO and LUMO orbitals with α -spin for **1**. HOMO – 2 HOMO – 1 HOMO LUMO LUMO + 1 LUMO + 2.

of the triphenylphosphine or triphenylphosphine oxide ligands participates in the higher unoccupied orbitals.

3.5. Electronic spectra

The spin-allowed triplet–triplet electronic transitions calculated with the TD-DFT method for **1** and **2** are gathered in Tables 7 and 8. For the high energy part of the spec-

trum, only transitions with oscillator strengths larger than 0.020 are listed in Tables 7 and 8.

The investigated complexes are of large size; the numbers of basis functions are equal to 969 and 799 for **1** and **2**, respectively. The calculated electron transitions (110 and 100 for **1** and **2**) do not comprise all the experimental absorption bands. The UV–Vis spectrum was calculated to ~ 290 nm for **1**, and to 300 nm for complex **2**. Thus

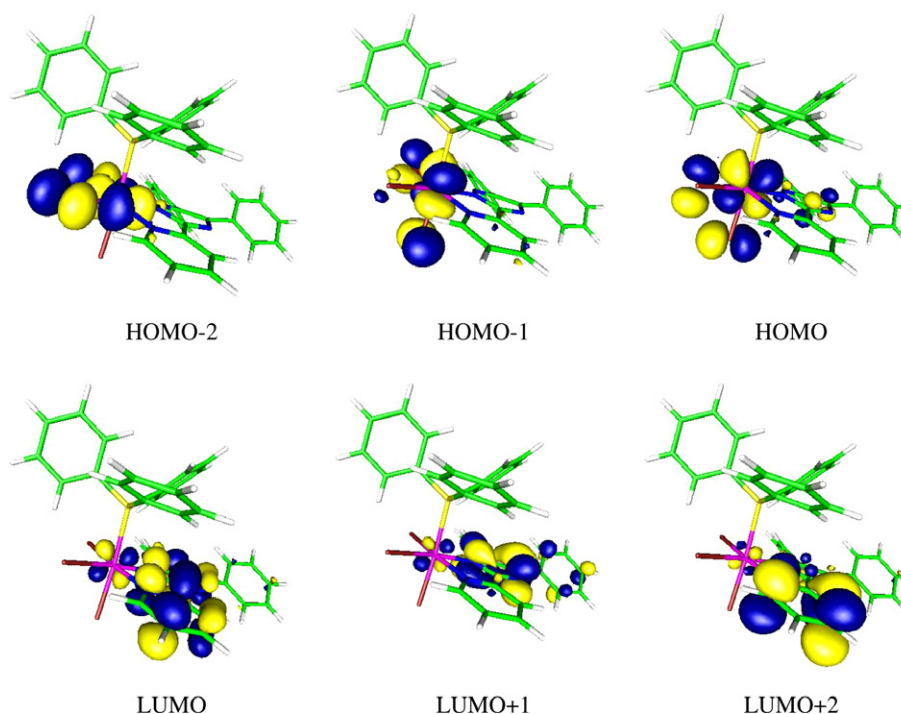


Fig. 4. The selected HOMO and LUMO orbitals with α -spin for **2**. HOMO – 2 HOMO – 1 HOMO LUMO LUMO + 1 LUMO + 2.

Table 7

The energy and molar absorption coefficients of experimental absorption bands and the electronic transitions calculated with the TD-DFT method for **1**

The most important orbital excitations	Character	λ (nm)	E (eV)	f	Experimental λ (nm) (E (eV)) ϵ
H(β) \rightarrow L + 3(β)	d \rightarrow d/ π^* (dppt)	929.2	1.33	0.0242	840.0 (1.48) 450 705.9 (1.76) 1150
H(α) \rightarrow L(α)	d \rightarrow π^* (dppt)	575.6	2.15	0.0227	
H(β) \rightarrow L + 6(β)	d \rightarrow d/ π^* (dppt)	514.6	2.41	0.0586	
H(β) \rightarrow L + 4(β)	d \rightarrow π^* (Ph _{OPPPh₃})				
H(α) \rightarrow L + 1(α)	d \rightarrow π^* (dppt)	502.1	2.47	0.0736	549.7 (2.26) 1700
H-1(α) \rightarrow L + 1(α)	d \rightarrow π^* (dppt)	481.6	2.57	0.0926	
H(β) \rightarrow L + 7(β)	d \rightarrow π^* (dppt)	443.3	2.80	0.0216	420.8 (2.95) 1070
H-5(β) \rightarrow L(β)	π (Ph _{OPPPh₃})/ π (Cl) \rightarrow π^* (dppt)	352.7	3.52	0.0247	
H-1(α) \rightarrow L + 4(α)	d \rightarrow (Ph _{OPPPh₃})				
H-1(β) \rightarrow L + 3(β)	π (Cl) \rightarrow d/ π^* (dppt)	345.8	3.59	0.0228	
H-3(α) \rightarrow L + 1(α)	π (Cl) \rightarrow π^* (dppt)	342.9	3.62	0.0618	328.3 (3.78) 5380
H-6(β) \rightarrow L + 1(β)	π (Ph _{OPPPh₃})/ π (Cl) \rightarrow d	334.0	3.71	0.0338	
H-1(β) \rightarrow L + 3(β)	π (Cl) \rightarrow d/ π^* (dppt)				
H-1(α) \rightarrow L + 3(α) H(β) \rightarrow L + 14(β)	d \rightarrow π^* (Ph _{OPPPh₃})	333.0	3.72	0.0315	
H-4(α) \rightarrow L(α)	π (dppt)/ π (Cl) \rightarrow π^* (dppt)	329.1	3.78	0.0243	
H(α) \rightarrow L + 2(α)	d \rightarrow π^* (Ph _{OPPPh₃})				
H(β) \rightarrow L + 15(β)	d \rightarrow π^* (Ph _{OPPPh₃})	321.5	3.86	0.0230	
H-1(α) \rightarrow L + 7(α)	d \rightarrow π^* (Ph _{OPPPh₃})	292.9	4.23	0.0210	274.0 (4.52) 9775 226.6 (5.47) 23650

ϵ , molar absorption coefficient ($\text{dm}^3 \text{mol}^{-1} \text{cm}^{-1}$); f , oscillator strength; H, highest occupied molecular orbital; L, lowest unoccupied molecular orbital.

the shortest wavelength experimental bands of **1** and **2** are not assigned to the calculated transitions; some additional intraligand and interligand transitions are expected to be found at higher energies in the calculations for **1** and **2**.

In the visible region (400–1000 nm), complexes **1** and **2** display multiple transitions of moderate intensity in the form of peaks and shoulders. The longest wavelength experimental band of **1** with maximum at 705.9 nm and

shoulder at 840 nm is very broad. It is assigned to the transition of d \rightarrow d/ π^* (dppt) character with relatively large oscillator strength. The calculated transition (at 929.2 nm) lies in the low energy end of the experimental band. For complex **2**, two absorption bands are observed in this range, and this arrangement is reproduced in the calculations. The experimental bands of **2** at 998.9 and 674.1 nm are attributed to the d \rightarrow d/ π^* (dppt) transitions

Table 8
The energy and molar absorption coefficients of experimental absorption bands and the electronic transitions calculated with the TD-DFT method for **2**

The most important orbital excitations	Character	λ (nm)	E (eV)	f	Experimental λ (nm) (E (eV)) ϵ
H(β) \rightarrow L + 1(β)	d \rightarrow d/ π^* (dppt)	976.3	1.27	0.0211	998.9 (1.24) 80
H(β) \rightarrow L + 3(β)	d \rightarrow d/ π^* (dppt)	806.0	1.54	0.0137	674.1 (1.84) 4400
H(α) \rightarrow L(α)	d \rightarrow d/ π^* (dppt)	562.0	2.21	0.0226	
H(α) \rightarrow L + 1(α)	d \rightarrow d/ π^* (dppt)	505.1	2.45	0.1167	520.3 (2.38) 5400
H-1(α) \rightarrow L + 1(α)	d \rightarrow d/ π^* (dppt)	486.4	2.55	0.0549	
H-5(β) \rightarrow L(β)	π (Cl)/ π (Ph _{PPH₃)/π(dppt) \rightarrow d/π^*(dppt)}	431.9	2.87	0.0225	432.9 (2.86) 4750
H-4(α) \rightarrow L + 1(α)	π (Cl)/ π (dppt) \rightarrow d/ π^* (dppt)	370.3	3.35	0.0427	
H-3(β) \rightarrow L(β)					
H-7(α) \rightarrow L(α)	π (Cl)/ π (Ph _{PPH₃)/π(dppt) \rightarrow d/π^*(dppt)}	356.6	3.48	0.0235	
H-5(α) \rightarrow L(α)					
H-3(α) \rightarrow L + 1(α)	π (Cl)/n(P)/ π (Ph _{PPH₃) \rightarrow d/π^*(dppt)}	354.6	3.50	0.0363	
H-3(β) \rightarrow L + 1(β)	π (Cl)/ π (dppt) \rightarrow d/ π^* (dppt)				
H-4(β) \rightarrow L + 1(β)	π (Cl)/ π (Ph _{PPH₃) \rightarrow d/π^*(dppt)}	345.2	3.59	0.0537	328.3 (3.78) 18240
H-7(α) \rightarrow L(α)	π (Cl)/ π (Ph _{PPH₃)/π(dppt) \rightarrow d/π^*(dppt)}	340.5	3.64	0.0474	
H-6(α) \rightarrow L(α)	π (Ph _{PPH₃) \rightarrow d/π^*(dppt)}	337.3	3.68	0.0664	
H-3(β) \rightarrow L + 3(β)	π (Cl)/ π (dppt) \rightarrow d/ π^* (dppt)				
H-7(β) \rightarrow L + 1(β)	π (Cl)/ π (dppt) \rightarrow d/ π^* (dppt)	317.6	3.90	0.0299	
H-8(α) \rightarrow L(α)	π (dppt) \rightarrow d/ π^* (dppt)				
H-12(β) \rightarrow L + 2(β)	π (Cl)/ π (PPh ₃)/ π (dppt) \rightarrow d	316.1	3.92	0.0250	
H(α) \rightarrow L + 4(α)	d \rightarrow π^* (Ph _{PPH₃)}				
					300.0 (4.13) 23200
					258.5 (4.80) 23680
					228.2 (5.43) 38850

calculated at 976.3 and 806.0 nm. The same character [d \rightarrow d/ π^* (dppt)] have the experimental absorption bands at 549.7 nm for complex **1** and at 520.3 nm for complex **2**. The observed shift of the d \rightarrow d/ π^* (dppt) bands to higher energy in going from triphenylphosphine oxide (**1**) to triphenylphosphine (**2**) coordination is consistent with the stabilization of the t_{2g} shell of complex **2** via back-bonding.

Some differences can be noticed in the assignment of the experimental absorption bands at 420.8 nm and 432 nm for **1** and **2**, respectively. The first one is assigned to the d \rightarrow d/ π^* (dppt) transition, whereas the absorption band of complex **2** corresponds to ligand–ligand charge transfer (π (Cl)/ π (PPh₃)/ π (dppt) \rightarrow d/ π^* (dppt)) transitions.

For both complexes the absorption bands below 400 nm are attributed to metal–ligand charge transfer, ligand–metal charge transfer and ligand–ligand charge transfer and interligand (IL) transitions (Tables 7 and 8).

3.6. Magnetic properties

The magnetic properties of **1** complex under the form μ_{eff} versus T (μ_{eff} the effective magnetic moment) is shown in Fig. 5. The chloro-derivative of the rhenium(III) shows room temperature magnetic moment 2.01 BM ($0.502 \text{ cm}^3 \text{ mol}^{-1} \text{ K}$). The magnetic moment of the solid is temperature independent between 300 and 60 K. In the temperature range 55–14 K it is observed only slightly

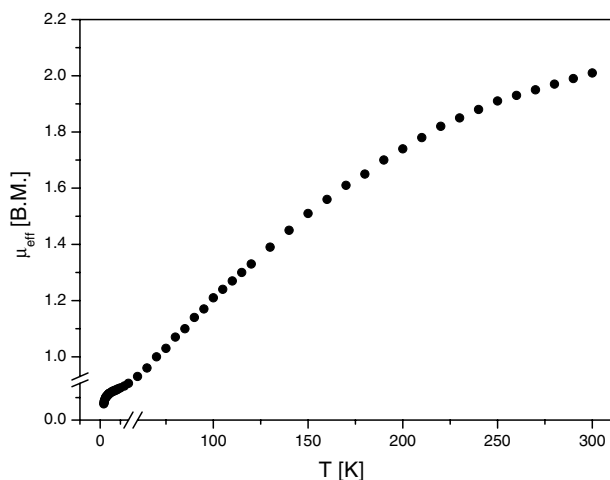


Fig. 5. Plots of the experimental effective magnetic moment μ_{eff} (●) vs. temperature for complex **1**.

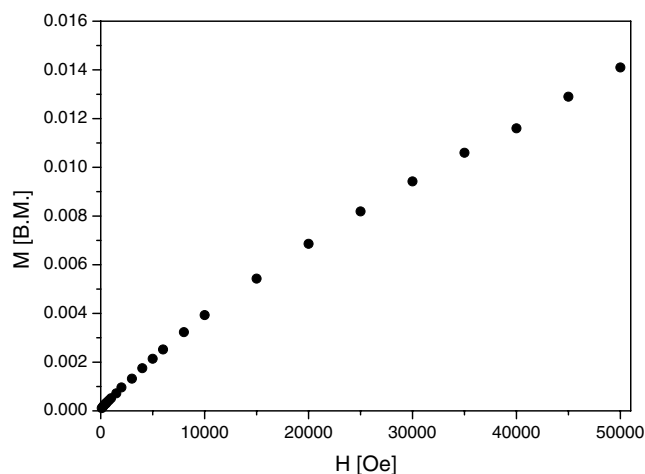


Fig. 6. Field dependence of the magnetization for complex **1** at 2 K.

magnetic anomaly and below 14 K the value of χ_M product increases with temperature lowering. This behavior is characteristic of mononuclear complexes with d^4 low-spin octahedral Re(III) complexes ($^3T_{1g}$ ground state) [30–38] and arise because of the large spin–orbit coupling ($\zeta = 2500 \text{ cm}^{-1}$ [39]), which gives diamagnetic ground state. It seems that in room temperature, in accordance Boltzmann's distribution, it is populated higher magnetic state, which is depopulated with temperature lowering and decreasing of the magnetic moment is observed.

The variation of the magnetization M versus the magnetic field H for complex **1** at 2 K is shown in Fig. 6. The M versus H curve for complex very slowly increases and indicates value of the magnetization near zero (0.014 BM) at 5 T. Magnetization of the sample confirms that the ground state is diamagnetic.

4. Supplementary material

CCDC 640907 and 640908 contain the supplementary crystallographic data for $\text{C}_{39}\text{H}_{31}\text{Cl}_5\text{N}_4\text{OPRe}$ and $\text{C}_{38}\text{H}_{29}\text{Cl}_3\text{N}_4\text{Pr}$. These data can be obtained free of charge via <http://www.ccdc.cam.ac.uk/conts/retrieving.html>, or from the Cambridge Crystallographic Data Centre, 12 Union Road, Cambridge CB2 1EZ, UK; fax: (+44) 1223-336-033; or e-mail: deposit@ccdc.cam.ac.uk.

Acknowledgements

The GAUSSIAN-03 calculations were carried out in the Wrocław Centre for Networking and Supercomputing, WCSS, Wrocław, Poland. The work was supported by the Polish Ministry of Science and Higher Education Grant No. 1T09A12430.

References

- [1] R.H. Holm, *Chem. Rev.* 87 (1987) 1401.
- [2] C.C. Romão, F.E. Kühn, W.A. Hermann, *Chem. Rev.* 97 (1997) 3197.
- [3] S.B. Seymore, S.N. Brown, *Inorg. Chem.* 39 (2000) 325.
- [4] W. Volkert, W.F. Goeckeler, G.J. Ehrhardt, A.R. Ketring, *J. Nucl. Med.* 32 (1991) 174.
- [5] E.A. Deutsch, K. Libson, J.L. Vanderheyden, *Technetium and Rhenium in Chemistry and Nuclear Medicine*, Raven Press, New York, 1990.
- [6] B. Machura, *Coord. Chem. Rev.* 249 (2005) 591.
- [7] H. Chermette, *Coord. Chem. Rev.* 178–180 (1998) 699.
- [8] M.C. Aragoni, M. Arca, T. Cassano, C. Denotti, F.A. Devillanova, F. Isaia, V. Lippolis, D. Natali, L. Niti, M. Sampietro, R. Tommasi, G. Verani, *Inorg. Chem. Commun.* 5 (2002) 869.
- [9] P. Romaniello, F. Lelj, *Chem. Phys. Lett.* 372 (2003) 51.
- [10] P. Norman, P. Cronstrand, J. Ericsson, *Chem. Phys.* 285 (2002) 207.
- [11] G. Rouschias, G. Wilkinson, *J. Chem. Soc. A* (1966) 465.
- [12] (a) CrysAlis RED, Oxford Diffraction Ltd., Version 1.171.29.2.; (b) STOE & Cie, X-RED: Version 1.18, STOE & Cie GmbH, Darmstadt, Germany, 1999.
- [13] G.M. Sheldrick, *Acta Crystallogr., Sect. A* 46 (1990) 467.
- [14] G.M. Sheldrick, *SHELXL-97: Program for the Refinement of Crystal Structures*, University of Göttingen, Göttingen, Germany, 1997.
- [15] G.M. Sheldrick, *SHELXTL: release 4.1 for Siemens Crystallographic Research Systems*, 1990.
- [16] M.J. Frisch, G.W. Trucks, H.B. Schlegel, G.E. Scuseria, M.A. Robb, J.R. Cheeseman, J.A. Montgomery Jr., T. Vreven, K.N. Kudin, J.C. Burant, J.M. Millam, S.S. Iyengar, J. Tomasi, V. Barone, B. Mennucci, M. Cossi, G. Scalmani, N. Rega, G.A. Petersson, H. Nakatsuji, M. Hada, M. Ehara, K. Toyota, R. Fukuda, J. Hasegawa, M. Ishida, T. Nakajima, Y. Honda, O. Kitao, H. Nakai, M. Klene, X. Li, J.E. Knox, H.P. Hratchian, J.B. Cross, C. Adamo, J. Jaramillo, R. Gomperts, R.E. Stratmann, O. Yazyev, A.J. Austin, R. Cammi, C. Pomelli, J.W. Ochterski, P.Y. Ayala, K. Morokuma, G.A. Voth, P. Salvador, J.J. Dannenberg, V.G. Zakrzewski, S. Dapprich, A.D. Daniels, M.C. Strain, O. Farkas, D.K. Malick, A.D. Rabuck, K. Raghavachari, J.B. Foresman, J.V. Ortiz, Q. Cui, A.G. Baboul, S. Clifford, J. Cioslowski, B.B. Stefanov, G. Liu, A. Liashenko, P. Piskorz, I. Komaromi, R.L. Martin, D.J. Fox, T. Keith, M.A. Al-Laham, C.Y. Peng, A. Nanayakkara, M. Challacombe, P.M.W. Gill, B. Johnson, W. Chen, M.W. Wong, C. Gonzalez, J.A. Pople, *GAUSSIAN-03, Revision B.03*, Gaussian, Inc., Pittsburgh, PA, 2003.
- [17] A.D. Becke, *J. Chem. Phys.* 98 (1993) 5648.
- [18] C. Lee, W. Yang, R.G. Parr, *Phys. Rev. B* 37 (1988) 785.
- [19] M.E. Casida, in: J.M. Seminario (Ed.), *Recent Developments and Applications in Modern Density Functional Theory, Theoretical and Computational Chemistry*, vol. 4, Elsevier, Amsterdam, 1996.
- [20] P.J. Hay, W.R. Wadt, *J. Chem. Phys.* 82 (1985) 299.
- [21] E. König, *Magnetic Properties of Coordination and Organometallic Transition Metal Compounds*, Springer, Berlin, 1966.
- [22] I. Chakraborty, S. Bhattacharyya, S. Banerjee, B.K. Dirghangi, A. Chakravorty, *J. Chem. Soc., Dalton Trans.* (1999) 3747.
- [23] S. Sengupta, J. Gangopadhyay, A. Chakravorty, *Dalton Trans.* (2003) 4635.
- [24] S. Das, I. Chakraborty, A. Chakravorty, *Polyhedron* 22 (2003) 901.
- [25] J. Gangopadhyay, S. Sengupta, S. Bhattacharyya, I. Chakraborty, A. Chakravorty, *Inorg. Chem.* 41 (2002) 2616.
- [26] K. Nakamoto, *Infrared and Raman Spectra of Inorganic and Coordination Compounds*, 4th ed., Wiley–Interscience, New York, 1986.
- [27] L.E. Helberg, S.D. Orth, M. Sabat, W.D. Harman, *Inorg. Chem.* 35 (1996) 5584.
- [28] J. Rall, F. Weingart, D.M. Ho, M.J. Heeg, F. Tisato, E. Deutsch, *Inorg. Chem.* 33 (1994) 3442.
- [29] S.D. Orth, J. Barrerra, M. Sabat, W.D. Harman, *Inorg. Chem.* 33 (1994) 3026.
- [30] J.E. Fergusson, *Coord. Chem. Rev.* 1 (1966) 459.
- [31] B.N. Figgis, J. Lewis, *Prog. Inorg. Chem.* 6 (1964) 37.
- [32] B.N. Figgis, *Introduction to Ligand Field*, Wiley–Interscience, New York, 1966, p. 248.
- [33] J. Chatt, G.J. Leigh, D.M.P. Mingos, E.W. Randall, D. Shaw, *J. Chem. Soc., Chem. Commun.* (1968) 419.
- [34] H.P. Gunz, G.J. Leigh, *J. Chem. Soc.* (1971) 2229.
- [35] B. Coutinho, J.R. Dilworth, P. Jobanputra, R.M. Thompson, S. Schmidt, J. Strähle, C.M. Archer, *J. Chem. Soc., Dalton Trans.* (1995) 1663.
- [36] M. Hirsch-Kuchma, T. Nicholson, A. Davison, W.M. Davis, A.G. Jones, *Inorg. Chem.* 36 (1997) 3237.
- [37] C.A. McConnachie, E.I. Stiefel, *Inorg. Chem.* 36 (1997) 6144.
- [38] C. Pearson, A.L. Beauchamp, *Can. J. Chem.* 75 (1997) 220.
- [39] A. Earnshaw, B.N. Figgis, J. Lewis, R.D. Peacock, *J. Chem. Soc.* (1961) 3132.